

Pion structure function and SU(2) flavor asymmetry*

Chueng-Ryong Ji[†]

North Carolina State University

Email: crji@ncsu.edu

We refine the computation of the $\bar{d} - \bar{u}$ flavor asymmetry in the proton sea with a complementary effort to reveal the dynamics of pion exchange in high-energy processes. In particular, we discuss the efficacy of pion exchange models to simultaneously describe leading neutron electroproduction at HERA along with the $\bar{d} - \bar{u}$ flavor asymmetry in the proton. A detailed χ^2 analysis of the ZEUS and H1 cross sections, when combined with constraints on the pion flux from Drell-Yan data, allows regions of applicability of one-pion exchange to be delineated. The analysis disfavors several models of the pion flux used in the literature, and yields an improved extraction of the pion structure function and its uncertainties at parton momentum fractions in the pion of $4 \times 10^{-4} \lesssim x_\pi \lesssim 0.05$ at a scale of $Q^2 = 10 \text{ GeV}^2$. Based on the fit results, we also address a possible estimate for leading proton structure functions in upcoming tagged deep-inelastic scattering experiments at Jefferson Lab on the deuteron with forward protons.

QCD Evolution 2016

May 30/June 03, 2016

National Institute for Subatomic Physics (Nikhef) in Amsterdam

*This work was in collaboration with **Joshua McKenney**, **Nobuo Sato** and **Wally Melnitchouk**, and was supported by the DOE contract No. DE-AC05-06OR23177, under which Jefferson Science Associates, LLC operates Jefferson Lab, and DOE Contract No. DE-FG02-03ER41260.

[†]Speaker.

1. Introduction

In this talk, we discuss our refined computation of the $\bar{d} - \bar{u}$ flavor asymmetry in the proton sea with a complementary effort to reveal the dynamics of pion exchange in high-energy processes. This complementary effort has been the study of leading neutron production in semi-inclusive deep inelastic scattering (DIS) on the proton, in which a forward moving neutron is produced in coincidence with the scattered lepton in the high-energy reaction $ep \rightarrow enX$. Several dedicated experiments at the ep collider HERA [1, 2, 3] have collected high-precision data on the spectrum of leading neutrons carrying a large fraction of the proton's energy. Moreover, the upcoming tagged DIS (TDIS) experiment at Jefferson Lab [4] plans to take data on the production of leading protons from an effective neutron target in the reaction $en \rightarrow epX$, which, in analogy with the HERA leading neutron leptonproduction, can be described through the exchange of a π^- . In the proposed experiment, the effective neutron target will be prepared by tagging spectator protons with momenta between 60 MeV and 400 MeV at backward kinematics in the DIS of the electron from a deuteron nucleus, using the same technique that was developed for the measurement of the neutron structure function in the BONuS experiment at Jefferson Lab [5].

In particular, we have recently addressed [6] the question of whether one can reduce the model dependence of F_2^π extracted from the HERA data [1, 2, 3] by using additional constraints from the data on the SU(2) flavor asymmetry $\bar{d} - \bar{u}$, especially those from the E866 Drell-Yan experiment [7]. Because the E866 data are at relatively high x values compared with the HERA measurements, within the pion exchange framework they are sensitive to the pion PDFs at large x_π , where these are well determined from pion-nucleon Drell-Yan data [8, 9, 10]. The main variable in describing the $\bar{d} - \bar{u}$ asymmetry is therefore the pion distribution function in the nucleon. In our study [6], we use methodology adopted from global PDF analysis [11, 12] to simultaneously fit both the HERA leading neutron and E866 $\bar{d} - \bar{u}$ asymmetry data. This study allows us to refine the analysis of the $\bar{d} - \bar{u}$ asymmetry and at the same time discuss a possible prediction of the future tagged DIS (TDIS) experiments in JLab.

2. Pion exchange models

In this section we briefly review the computation of the pion light-cone momentum distributions in the nucleon (sometimes also referred to as the pion splitting functions), for both πN and $\pi\Delta$ fluctuations of the proton.

For the fluctuation of a proton (with four momentum p) to a positively charged pion (momentum k) and a neutron ($p - k$), illustrated by the “rainbow” diagram in Fig. 1 (a), the $p \rightarrow n\pi^+$ splitting function derived from chiral effective theory is expressed as a sum of on-shell and δ -function pieces [13, 14],

$$f_{\pi^+n}(y) = 2 \left[f_N^{(\text{on})}(y) + f_N^{(\delta)}(y) \right], \quad (2.1)$$

where $y = k^+/p^+$ is the fraction of the proton's light-cone momentum carried by the pion, and the “+” component of the four-vector is defined as $k^+ \equiv k^0 + k^z$. The on-shell contribution $f_N^{(\text{on})}$ corresponds to the region $y > 0$ and can be written as [15, 16]

$$f_N^{(\text{on})}(y) = \frac{g_A^2 M^2}{(4\pi f_\pi)^2} \int dk_\perp^2 \frac{y(k_\perp^2 + y^2 M^2)}{(1-y)^2 D_{\pi N}^2}, \quad (2.2)$$

where M is the nucleon mass, $g_A = 1.267$ is the axial charge, $f_\pi = 93$ MeV is the pion decay constant, and

$$D_{\pi N} \equiv t - m_\pi^2 = -\frac{1}{1-y} [k_\perp^2 + y^2 M^2 + (1-y)m_\pi^2] \quad (2.3)$$

for an on-shell nucleon intermediate state, with the pion virtuality $t \equiv k^2 = -(k_\perp^2 + y^2 M^2)/(1-y)$. The second term in Eq. (2.1), $f_N^{(\delta)}$, arises from off-shell nucleon contributions and is proportional to $\delta(y)$. The significance of this term has been discussed [17] with respect to the model-independent nonanalytic structure of the vertex renormalization constant as a function of the pion mass. One may regard this nonanalytic function of m_π^2 as the first principles constraint on the infrared behavior of the chiral effective theory consistent with the chiral symmetry of QCD. In scattering processes this term contributes only at $x = 0$, and is therefore relevant only for the lowest moment of the parton distribution. In the work of analyzing data at nonzero values of x , $f_N^{(\delta)}$ plays no direct role.

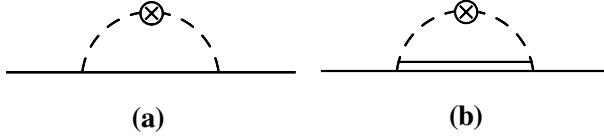


Figure 1: Contributions to the pion distributions in the proton from the rainbow diagrams involving (a) a nucleon (solid lines) and (b) a Δ isobar (double solid line) in the intermediate state. The external operators couple to the virtual pions (dashed lines).

Note that the factor 2 in Eq. (2.1) is an isospin factor specific to the $p \rightarrow n\pi^+$ fluctuation; the distribution for the fluctuation $p \rightarrow p\pi^0$ is related to that in Eq. (2.1) by $f_{\pi^+n}(y) = 2f_{\pi^0p}(y)$. In writing the coefficient in front of the integration in Eq. (2.2), we have assumed the Goldberger-Treiman relation, $g_A/f_\pi = g_{\pi NN}/M$, where $g_{\pi NN}^2/4\pi \approx 13.7$ gives the strength of the πNN coupling [18].

In addition to the nucleon intermediate states, contributions from Δ baryons in Fig. 1 (b) are known to play an important role in hadron structure. Within the same chiral effective theory framework, using an effective $\pi N\Delta$ interaction [14], the $p \rightarrow \Delta^0 \pi^+$ splitting function can be written as a sum of three terms,

$$f_{\pi^+\Delta^0}(y) = f_\Delta^{(\text{on})}(y) + f_\Delta^{(\delta)}(y) + f_\Delta^{(\text{end-pt})}(y). \quad (2.4)$$

The on-shell piece $f_\Delta^{(\text{on})}$, corresponding to the Δ pole, is given for $0 < y < 1$ by

$$f_\Delta^{(\text{on})}(y) = C_\Delta \int dk_\perp^2 \frac{y(\bar{M}^2 - m_\pi^2)}{(1-y)D_{\pi\Delta}^2} \left[(\bar{M}^2 - m_\pi^2)(\Delta^2 - m_\pi^2) - [3(\Delta^2 - m_\pi^2) + 4MM_\Delta]D_{\pi\Delta} \right] \quad (2.5)$$

where

$$D_{\pi\Delta} \equiv t - m_\pi^2 = -\frac{1}{1-y} [k_\perp^2 - y(1-y)M^2 + yM_\Delta^2 + (1-y)m_\pi^2] \quad (2.6)$$

for an on-shell Δ intermediate state of mass M_Δ , with $\bar{M} \equiv M_\Delta + M$ and $\Delta \equiv M_\Delta - M$. The pion virtuality here is given by $t \equiv k^2 = -(k_\perp^2 - y(1-y)M^2 + yM_\Delta^2)/(1-y)$. The coefficient $C_\Delta = g_{\pi N\Delta}^2/[(4\pi)^2 18M_\Delta^2]$ contains the $\pi N\Delta$ coupling constant, which is given from $SU(6)$ symmetry by $g_{\pi N\Delta} = (3\sqrt{2}/5)g_A/f_\pi \approx 11.8$ GeV $^{-1}$ [20]. For the other charge channels in the $p \rightarrow \Delta\pi$ dissociation, the splitting functions are related by $2f_{\pi^-\Delta^+} = 3f_{\pi^0\Delta^+} = 6f_{\pi^+\Delta^0}$.

Note that the on-shell contribution in Eq. (2.5) differs from the ‘‘Sullivan’’ form often used in the literature [19, 20, 21, 22], which is obtained by taking the Δ -pole contribution, $D_{\pi\Delta} \rightarrow M_{\Delta}^2$. In particular, it has a higher power of k_{\perp} (k_{\perp}^6 compared with k_{\perp}^2 in Eq. (2.5)), which arises from the neglect of the end-point contributions in the Sullivan process. The other two terms in Eq. (2.4), $f_{\Delta}^{(\delta)}$ and $f_{\Delta}^{(\text{end-pt})}$, correspond to a δ -function contribution at $y = 0$ and an end-point contribution proportional to a δ -function at $y = 1$, respectively.

From the on-shell nucleon and Δ splitting functions in Eqs. (2.2) and (2.5), it is evident that integration over contributions from large k_{\perp} will introduce logarithmic divergences in the point-like theory, which must be regularized in order to obtain finite results. Since the nucleon is not point-like, but has a finite spatial extent of $\mathcal{O}(1 \text{ fm})$, this introduces an additional scale into the effective theory, along with the chiral symmetry breaking scale [23]. The precise way that the finite range of the nucleon is implemented in order to regularize the ultraviolet divergences depends on the prescription adopted [23, 24], although any prescription must correctly incorporate the infrared behavior of pion loops which is model independent. In practice, the model dependence amounts to a choice of form factor $F(y, k_{\perp}^2)$ multiplying the integrands of Eqs. (2.2) and (2.5) which suppresses the large- k_{\perp} contributions. In our recent paper [6], we have extensively discussed the available regularization prescriptions and noted that the best results for the E866 data were obtained with the t -dependent exponential form factor given by

$$F = \exp[(t - m_{\pi}^2)/\Lambda^2] \quad [t\text{-dependent exponential}], \quad (2.7)$$

where the best fit values of the ultraviolet cutoff parameter Λ were found as $\Lambda \approx 0.85(0.88) \text{ GeV}$ with the SMRS [25] (ASV [26]) parametrization for the pion PDFs.

3. SU(2) flavor asymmetry of the sea

The E866 experiment at Fermilab measured the ratio σ^{pd}/σ^{pp} at high (projectile) proton momentum fractions x_1 and low target momentum fraction x_2 , where at leading order in the strong coupling constant α_s it is approximately given by [7]

$$\frac{\sigma^{pd}}{2\sigma^{pp}} \approx \frac{1}{2} \left(1 + \frac{\bar{d}(x_2)}{\bar{u}(x_2)} \right), \quad [x_1 \gg x_2]. \quad (3.1)$$

The cross sections were measured for x_2 between 0.015 and 0.35, at an average dimuon mass squared of $Q^2 = 54 \text{ GeV}^2$, and the extracted \bar{d}/\bar{u} ratio was found to exceed 1.5 for $x_2 \approx 0.1 - 0.2$.

We have examined [6] the constraints on the models of the pion cloud of the nucleon that can be inferred from a detailed analysis of the $\bar{d} - \bar{u}$ asymmetry in the proton. Within the effective chiral framework described in Sec. 2, the contributions to the $\bar{d} - \bar{u}$ difference from the pion loop diagrams in Fig. 1 can be written as [14]

$$\bar{d} - \bar{u} = \left(f_{\pi^+n} - \frac{2}{3} f_{\pi^-\Delta^{++}} \right) \otimes \bar{q}_v^{\pi}, \quad (3.2)$$

where $\bar{q}_v^{\pi} \equiv \bar{d}^{\pi^+} - d^{\pi^+} = \bar{u}^{\pi^-} - u^{\pi^-}$ is the valence quark PDF in the \bar{u} pion, and the symbol ‘‘ \otimes ’’ denotes the convolution integral $f \otimes q = \int_0^1 dy \int_0^1 dz f(y) q(z) \delta(x - yz)$. This convolution expression (3.2) is the standard one used in calculations of chiral loop corrections in meson cloud models

and its appearance in the effective chiral theory is made manifest recently [27]. As we discuss the efficacy of the pion exchange model [6] in Sec. 4, we focus on the kinematic region where it is natural to treat the peripheral modification of the nucleon in terms of pions [28]. The convolution in Eq. (3.2) follows from the crossing symmetry properties of the splitting functions $f(-y) = f(y)$ [29], and isospin symmetry relations have been assumed for the $\pi\Delta$ distributions. The contributions from neutral pions cancel in the asymmetry.

Performing a χ^2 fit to the E866 data, we have compared the results for the various regularization prescriptions with the best fit cutoff parameters and χ_{dof}^2 values [6]. For the valence antiquark distribution in the pion we used the SMRS parametrization [25] of the world's data from πN Drell-Yan and prompt photon production, evaluated at the E866 average Q^2 of 54 GeV². As indicated in Sec. 2, the fits with the lowest χ_{dof}^2 values were obtained with the t -dependent exponential regulator [Eq. (2.7)]. For much greater details including the analyses of other comparable regularizations, one should take a look at our recent paper [6]. We note that the biggest contributions to the χ^2 arise from the high- x data points, which have a steeper fall-off than can be accommodated in any of the models. We anticipate that the new SeaQuest experimental result at Fermilab [30] will in the near future check the high- x behavior of the \bar{d}/\bar{u} ratio more stringently up to $x \approx 0.45$.

While the pion PDFs at small x values have never been directly measured, in the valence quark region the πN Drell-Yan data [8, 9, 10] provide strong constraints on the x dependence of \bar{q}_v^π for $x \gtrsim 0.1$. Interestingly, the distributions at $x \rightarrow 1$ were observed [10] to be more consistent with a $\sim (1-x)$ behavior [31, 32, 33] than with the $\sim (1-x)^2$ expectation from perturbative QCD [34] or model calculations using the Dyson-Schwinger equations (see Ref. [35]). The large- x behavior in the SMRS parametrization [25] was consistent with the $\sim (1-x)$ form indicated by the data.

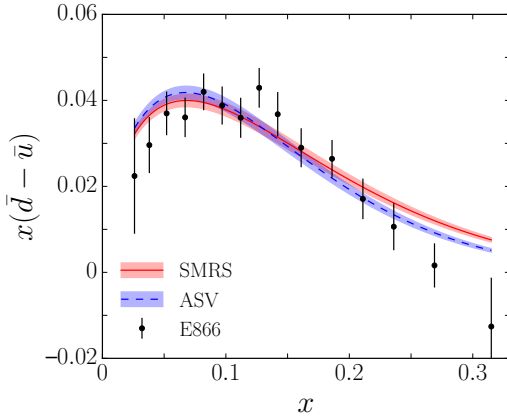


Figure 2: Comparison of the pion model fits to the $\bar{d} - \bar{u}$ data from the E866 experiment [7] with the t -dependent exponential form factor (2.7) for the valence pion PDFs from the SMRS [25] and ASV [26] parametrizations.

Later, an analysis including next-to-leading order (NLO) corrections [36] found that the higher order effects soften the distributions, leading to a behavior that was intermediate between $(1-x)$ and $(1-x)^2$. More recently, Aicher *et al.* (ASV) [26] found that inclusion of threshold resummation at next-to-leading log (NLL) accuracy produces valence distributions that behave approximately as $(1-x)^2$ at a low energy scale $Q_0 = 0.63$ GeV.

In order to assess the possible impact of the different $x \rightarrow 1$ behaviors of the valence pion PDF on the $\bar{d} - \bar{u}$ asymmetry, we repeated our analysis using the ASV parametrization [26], evolved from the low energy scale Q_0 to $Q^2 = 54$ GeV². The best fit results are compared in Fig. 2 for

the t -dependent exponential form factor (2.7) with the result using the SMRS parametrization. As expected, the result with the ASV distribution leads to a softer asymmetry, with slightly better agreement at large x but marginally worse at $x \lesssim 0.1$. The overall χ^2_{dof} values are slightly better for the ASV fit, mostly because the softer distribution allows a smaller asymmetry at $x \gtrsim 0.2$, as preferred by the E866 data, although the differences are not significant. The new results for the flavor asymmetry from the SeaQuest experiment [30] at large x will provide further insights into these comparisons.

4. Efficacy of the pion exchange model in leading neutron production at HERA

We have examined [6] the efficacy of the pion exchange model described in Sec. 3 in fitting the HERA leading neutron production data [1, 2], and the compatibility of the results with the $\bar{d} - \bar{u}$ asymmetry extracted from the E866 Drell-Yan measurement [7]. While some dedicated analyses [37] have attempted to describe the HERA leading neutron spectra at all kinematics, our aim here was instead to maximize the sensitivity to the basic one-pion exchange contribution, which has the most direct connection to the chiral effective theory. This has been achieved by restricting the analysis to regions where one-pion exchange is expected to be the dominant process, and contributions from other backgrounds are minimal. In practice, since the calculation of the backgrounds is significantly more model dependent, the exact choice of kinematics may be somewhat subjective. To determine in a more objective way the region of kinematics where the one-pion exchange is applicable, we performed a χ^2 analysis of the data as a function of the maximum value of y up to which the data were fitted, i.e. $y < y_{\text{cut}}$. Although this reduced the total number of data points in the fit, the analysis of the more restrictive kinematic range allowed for a cleaner interpretation and extraction of the pion exchange parameters.

The tagged neutron structure function $F_2^{\text{LN}(3)}$ extracted from the differential cross section for the production of leading neutrons (LN) in semi-inclusive ep scattering can be written as [6]

$$F_2^{\text{LN}(3)}(x, Q^2, y) = 2f_N^{(\text{on})}(y)F_2^\pi(x_\pi, Q^2), \quad (4.1)$$

where $f_N^{(\text{on})}(y)$ is given by Eq.(2.2) and $F_2^\pi(x_\pi, Q^2)$ is the pion structure function. The H1 experiment [2] measured $F_2^{\text{LN}(3)}$ over a large range of kinematics covering $1.5 \times 10^{-4} \leq x \leq 3 \times 10^{-2}$ and $6 \leq Q^2 \leq 100 \text{ GeV}^2$ for average y values between 0.05 and 0.68. A similarly extensive range of kinematics was covered by the ZEUS data [1]. Taking the t -dependent exponential model with $y_{\text{cut}} = 0.3$ as the optimal result of our fits, we obtained the spectra of leading neutrons from the ZEUS [1] and H1 [2] experiments, as shown in Figs. 3 and 4, respectively.

With the inclusion of the E866 $\bar{d} - \bar{u}$ asymmetry data in the fits together with the HERA leading neutron cross sections, the correlations between the pion flux and pion structure function parameters decreased dramatically for all cutoff models. For the t -dependent exponential model (2.7), the correlations between the Λ parameter and the normalization parameter of the pion structure function were reduced to between -8% to -16% over the range of cutoffs between $y_{\text{cut}} = 0.1$ and 0.4 . There was significantly greater discriminating power between the form factor models, with much stronger dependence of the fit results to the value of y_{cut} . It is interesting to note that the behavior of the t variable at small y is given by $t \sim -k_\perp^2/(1-y)$ so that any undesirable suppression at small

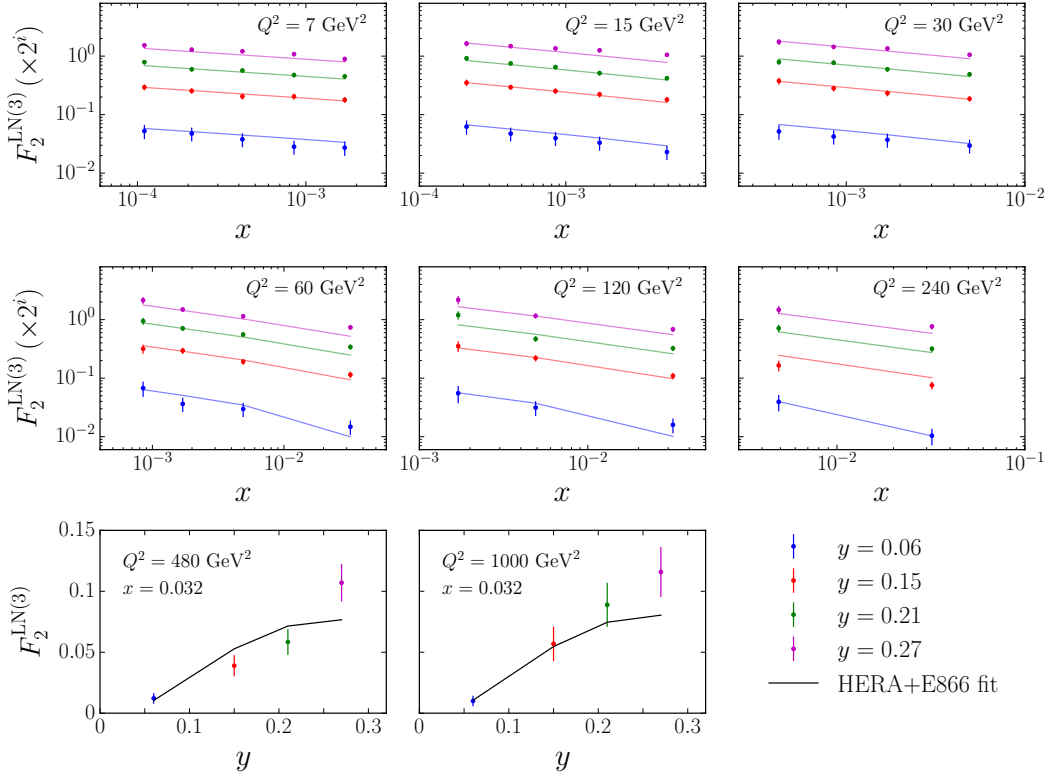


Figure 3: Leading neutron structure function $F_2^{\text{LN}(3)}$ from ZEUS [1] as a function of x at fixed values of Q^2 and y . The panels at $Q^2 = 480$ and 1000 GeV^2 are shown as a function of y for fixed $x = 3.2 \times 10^{-2}$. The fitted results have been computed for the t -dependent exponential model (2.7) with $y_{\text{cut}} = 0.3$. For clarity, the values of $F_2^{\text{LN}(3)}$ in the first six panels (for $Q^2 \leq 240 \text{ GeV}^2$) have been offset by multiplying by a factor 2^i for $i = 0$ (for $y = 0.06$) to $i = 3$ (for $y = 0.27$).

y such as the poor fit to the small- y HERA and E866 data does not occur for the t -dependent form factors. Through the convolution formula (3.2), one can see that less strength at small y also translates into suppression of the calculated PDFs at small x values. Again, for much greater details of this analysis, one should take a look at our recent paper [6].

5. Pion structure function at small x

Having systematically quantified the efficacy of the various pion exchange models in describing the HERA leading neutron and E866 $\bar{d} - \bar{u}$ asymmetry data, we now assess whether and to what extent the combined analysis is able to unambiguously determine the x_π dependence of the pion structure function. Choosing the t -dependent exponential model for the πNN form factor (2.7) as the one best capable of giving a consistent description of the data over the largest range of kinematics, in Fig. 5 (a) we illustrate the stability of the results for F_2^π with respect to the value of y_{cut} , at a fixed $Q^2 = 10 \text{ GeV}^2$. With the exception of the $y_{\text{cut}} = 0.1$ fit, the extracted F_2^π shows remarkable stability across all cuts up to the optimal $y_{\text{cut}} = 0.3$ and even beyond, over the entire range of $x_\pi \gtrsim 4 \times 10^{-4}$ constrained by the ZEUS and H1 data. Note that each of the curves is plotted for x_π down to different values of $x_\pi^{\text{min}} = x_{\text{min}}/y_{\text{cut}}$ because of the varying y_{cut} values in each fit.

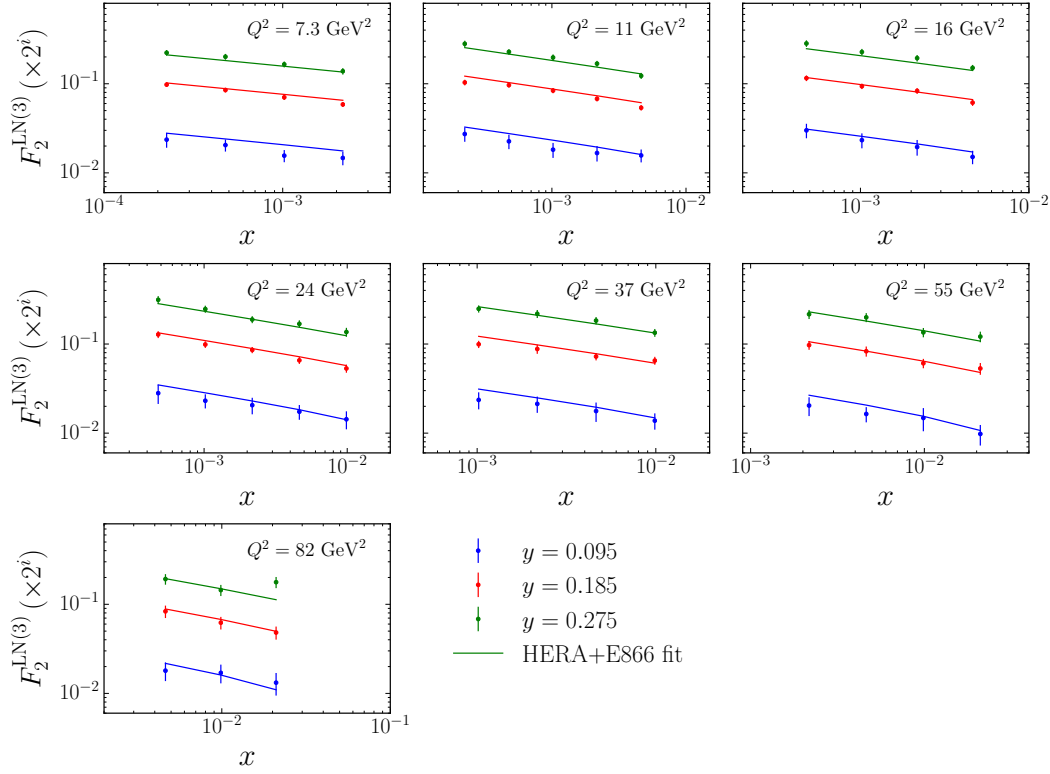


Figure 4: Leading neutron structure function $F_2^{\text{LN}(3)}$ from H1 [2] as a function of x at fixed values of Q^2 and y . The fitted results have been computed for the t -dependent exponential model (2.7) of the pion flux with $y_{\text{cut}} = 0.3$. For clarity, the values of $F_2^{\text{LN}(3)}$ have been offset by multiplying by a factor 2^i for $i = 0$ (for $y = 0.095$) to $i = 3$ (for $y = 0.275$).

Although the t -dependent exponential model gave the smallest χ_{dof}^2 of all models in the combined fit, up to $y_{\text{cut}} = 0.4$, the dependence of the fitted F_2^π on the functional form of the πNN form factor is rather weak, as Fig. 5 (b) illustrates for $y_{\text{cut}} = 0.3$. All the models listed in the legend of Fig. 5 (b) were defined in our recent paper [6]. Interestingly, the best fit model (2.7) gives the smallest F_2^π result.

For a given model, the propagated fit errors from the analysis are rather small as indicated by the band around the extracted F_2^π in Fig. 5 (c) where the t -dependent exponential model with $y_{\text{cut}} = 0.3$ was shown. The PDF error is also generally substantially smaller than the difference between our fitted result for F_2^π and the values from the SMRS [25] and GRS [38] global PDF analyses, extrapolated to the small- x region of HERA kinematics. In particular, while our extracted F_2^π has a similar shape to the GRS parametrization, its magnitude is $\approx 30\% - 40\%$ smaller at $x_\pi \approx 10^{-3} - 10^{-2}$. The magnitude is closer to the result from the SMRS parametrization at similar x_π values, but the latter shows considerably less variation with x_π . More detailed assessment on our extracted F_2^π can be found in our recent paper [6].

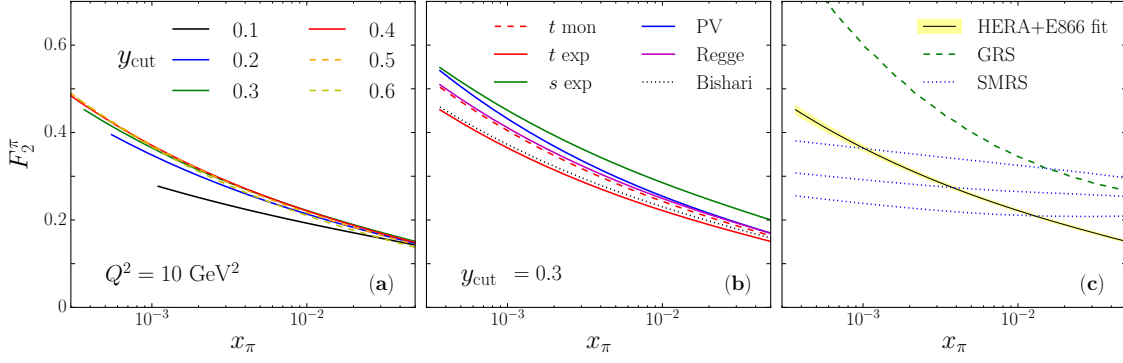


Figure 5: Pion structure function F_2^π as a function of x_π at $Q^2 = 10 \text{ GeV}^2$, extracted from a simultaneous fit to the ZEUS and H1 leading neutron data and the E866 $\bar{d} - \bar{u}$ asymmetry for (a) the t -dependent exponential model with different y_{cut} values, (b) various models at fixed y_{cut} , and (c) the best fit t -dependent exponential model with $y_{\text{cut}} = 0.3$, compared with the GRS [38] and SMRS [25] parametrizations, with the latter shown for a 10% (lowest), 15% (central) and 20% (highest) pion sea.

6. Future direction

Our analysis has sought to determine whether both the $\bar{d} - \bar{u}$ asymmetry in the proton extracted from the E866 Drell-Yan data [7] and the HERA leading neutron cross sections [1, 2, 3] can be obtained consistently within a common pion exchange framework. Rather than relying on assumptions about specific forms for the pion distributions in the nucleon, we have addressed the model dependence empirically, by performing the first comprehensive statistical analysis of the combined HERA leading neutron and E866 data sets, for a wide range of prescriptions adopted in the literature for regularizing the pion-nucleon amplitudes. Our findings suggest that we can indeed describe both HERA and E866 data within pion exchange models, if the cutoff parameters in the πNN form factors are fitted simultaneously with the pion structure function. The combined fits to both the HERA and E866 data are significantly more restrictive, with models with t -dependent form factors, such as exponential or monopole, giving the best descriptions of the combined data sets over the largest range of kinematics, up to $y_{\text{cut}} \approx 0.3$ [21, 22, 20].

In the near future, the new SeaQuest [30] experimental result on the $\bar{d} - \bar{u}$ difference up to $x \approx 0.45$ will allow improved constraints on the models of the pion distribution function in the nucleon. Beyond that, the TDIS experiment [4] at Jefferson Lab will provide precise information on pion exchange in leading proton production from an effective neutron target at kinematics complementary to the range covered by the HERA and Drell-Yan measurements. This should reduce the uncertainty in F_2^π in the intermediate x_π region, $x_\pi \sim 0.1$.

One may also examine in more detail the k_\perp dependence of leading neutron (or proton) cross sections, which was studied in some of the HERA measurements [3] and will be explored in the TDIS experiment. Comparison of the unintegrated pion flux with the empirical transverse momentum distributions could provide a more incisive test of the momentum dependence of the πNN form factor. In the longer term, a necessary goal would be to perform a global PDF fit, in terms of both sea and valence quark PDFs, to the πN Drell-Yan data at moderate and high values of x_π , together with HERA leading neutron data at small x_π , and the new TDIS data on leading proton production

in the intermediate x_π region. We look forward to these endeavors revealing much more consisely and completely the partonic structure of the pion, and the role of the pion cloud in the structure of the nucleon.

References

- [1] Chekanov,S., *et al.*: Leading neutron production in e^+p collisions at HERA, Nucl. Phys. B **637**, 3 (2002).
- [2] Aaron,F. D., *et al.*: Measurement of Leading Neutron Production in Deep-Inelastic Scattering at HERA, Eur. Phys. J. C **68**, 381 (2010).
- [3] Chekanov,S., *et al.*: Leading neutron energy and pT distributions in deep inelastic scattering and photoproduction at HERA Nucl. Phys. B **776**, 1 (2007).
- [4] Keppel,C., Wojtsekhowski,B., King,P., Dutta,D. and Annand,J. as spokespersons: Measurement of Tagged Deep-Inelastic Scattering (TDIS), Jefferson Lab experiment PR12-15-006.
- [5] Baillie,N., *et al.*: Measurement of the neutron F2 structure function via spectator tagging with CLAS, Phys. Rev. Lett. **108**, 142001 (2012).
- [6] McKenney,J. R., Sato,N., Melnitchouk,W. and Ji, C.-R.: Pion structure function from leading neutron electroproduction and $SU(2)$ flavor asymmetry, Phys. Rev. D **93**, 054011 (2016).
- [7] Towell,R.S., *et al.*: Improved measurement of the anti-d / anti-u asymmetry in the nucleon sea, Phys. Rev. D **64**, 052002 (2001).
- [8] Badier,J., *et al.*: Experimental Determination of the π Meson Structure Functions by the Drell-Yan Mechanism, Z. Phys. C **18**, 281 (1983).
- [9] Betev,B., *et al.*: Observation of Anomalous Scaling Violation in Muon Pair Production by 194-GeV/c π^- Tungsten Interactions, Z. Phys. C **28**, 15 (1985).
- [10] Conway,J.S., *et al.*: Experimental Study of Muon Pairs Produced by 252-GeV Pions on Tungsten, Phys. Rev. D **39**, 92 (1989).
- [11] Jimenez-Delgado,P., Melnitchouk,W. and Owens,J. F.: Parton momentum and helicity distributions in the nucleon, J. Phys. G **40**, 093102 (2013).
- [12] Forte,S. and Watt,G.: Progress in the Determination of the Partonic Structure of the Proton, Ann. Rev. Nucl. Part. Sci. **63**, 291 (2013).
- [13] Burkardt,M., Hendricks,K. S., Ji,C.-R., Melnitchouk,W. and Thomas,A. W.: Pion momentum distributions in the nucleon in chiral effective theory, Phys. Rev. D **87**, 056009 (2013).
- [14] Salamu,Y., Ji,C.-R., Melnitchouk,W. and Wang,P.: $\bar{d} - \bar{u}$ asymmetry in the proton in chiral effective theory, Phys. Rev. Lett. **114**, 122001 (2015).
- [15] Thomas,A. W.: A Limit on the Pionic Component of the Nucleon Through $SU(3)$ Flavor Breaking in the Sea, Phys. Lett. B **126**, 97 (1983).
- [16] Drell,S. D., Levy,D. J. and Yan,T. M.: A Theory of Deep Inelastic Lepton-Nucleon Scattering and Lepton Pair Annihilation Processes. 1., Phys. Rev. **187**, 2159 (1969).
- [17] Ji,C.-R., Melnitchouk,W. and Thomas,A. W.: Anatomy of relativistic pion loop corrections to the electromagnetic nucleon coupling, Phys. Rev. D **88**, 076005 (2013).

- [18] Bugg, D. V.: The pion nucleon coupling constant, *Eur. Phys. J. C* **33**, 505 (2004).
- [19] Thomas, A. W., Melnitchouk, W. and Steffens, F. M.: Dynamical symmetry breaking in the sea of the nucleon, *Phys. Rev. Lett.* **85**, 2892 (2000).
- [20] Melnitchouk, W., Speth, J. and Thomas, A. W.: Dynamics of light anti-quarks in the proton, *Phys. Rev. D* **59**, 014033 (1999).
- [21] Kumano, S.: Flavor asymmetry of anti-quark distributions in the nucleon, *Phys. Rep.* **303**, 183 (1998).
- [22] Speth, J. and Thomas, A. W.: Mesonic contributions to the spin and flavor structure of the nucleon, *Adv. Nucl. Phys.* **24**, 83 (1998).
- [23] Donoghue, J. F., Holstein, B. R. and Borasoy, B.: $SU(3)$ baryon chiral perturbation theory and long distance regularization, *Phys. Rev. D* **59**, 036002 (1999).
- [24] Young, R. D., Leinweber, D. B. and Thomas, A. W.: Leading quenching effects in the proton magnetic moment, *Phys. Rev. D* **71**, 014001 (2005);
- [25] Sutton, P. J., Martin, A. D., Roberts, R. G. and Stirling, W. J.: Parton distributions for the pion extracted from Drell-Yan and prompt photon experiments, *Phys. Rev. D* **45**, 2349 (1992).
- [26] Aicher, M., Schafer, A. and Vogelsang, W.: Soft-gluon resummation and the valence parton distribution function of the pion, *Phys. Rev. Lett.* **105**, 252003 (2010).
- [27] Wang, X. G., Ji, C.-R., Melnitchouk, W., Salamu, Y., Thomas, A. W. and Wang, P.: Strange quark asymmetry in the proton in chiral effective theory, ADP-16-35/T991; JLAB-THY-16-2367.
- [28] Llewellyn Smith, C. H.: Nuclear Effects in Deep Inelastic Lepton Scattering, *Nucl. Phys. A* **434**, 35c-56c (1985).
- [29] Chen, J.-W. and Ji, X.: Constructing parton convolution in effective field theory, *Phys. Rev. Lett.* **87**, 152002 (2001); *ibid* **88**, 249901(E) (2002).
- [30] Geesaman, D. F. and Reimer, P. E. as spokespersons: Fermilab E906 experiment (SeaQuest), <http://www.phy.anl.gov/mep/SeaQuest/>.
- [31] Melnitchouk, W.: Quark hadron duality in electron pion scattering, *Eur. Phys. J. A* **17**, 223 (2003); Melnitchouk, W.: Higher twists in the pion structure function, *Phys. Rev. D* **67**, 077502 (2003).
- [32] Shigetani, T., Suzuki, K. and Toki, H.: Pion structure function in the Nambu and Jona-Lasinio model, *Phys. Lett. B* **308**, 383 (1993).
- [33] Szczepaniak, A., Ji, C.-R. and Cotanch, S. R.: Generalized relativistic meson wave function, *Phys. Rev. D* **49**, 3466 (1994).
- [34] Farrar, G. R. and Jackson, D. R.: The Pion Form-Factor, *Phys. Rev. Lett.* **43**, 246 (1979).
- [35] Holt, R. J. and Roberts, C. D.: Distribution Functions of the Nucleon and Pion in the Valence Region, *Rev. Mod. Phys.* **82**, 2991 (2010).
- [36] Wijesooriya, K., Reimer, P. E. and Holt, R. J.: The pion parton distribution function in the valence region, *Phys. Rev. C* **72**, 065203 (2005).
- [37] Kopeliovich, B. Z., Potashnikova, I. K., Povh, B. and Schmidt, I.: Pion structure function at small x from DIS data, *Phys. Rev. D* **85**, 114025 (2012).
- [38] M. Glück, E. Reya and M. Stratmann, *Eur. Phys. J. C* **2**, 159 (1998).